Ecosystems (2016) 19: 1225–1239
DOI: 10.1007/s10021-016-9996-8

ECOSYSTEMS

Forest Structure Affects the Stoichiometry of Periphyton Primary Producers in Mountain Streams of Northern Patagonia

Nicolás Martyniuk,* Beatriz Modenutti, and Esteban Balseiro

Laboratorio de Limnologíal, INIBIOMA, CONICET-UN Comahue, Quintral 1250, 8400 Bariloche Rio Negro, Argentina

Abstract

Riparian zones are major components of stream ecosystems that influence the physical, chemical, and biological parameters. In particular, the distribution of vertical foliage and the structure of riparian vegetation determine light availability in canopied streams. Here, we analyzed how forest structure will modify light availability and thus affect primary producers' photosynthetic parameters and the periphyton stoichiometry of mountain streams. We carried out field sampling in four streams with different canopies located in the North-Patagonian Andes and conducted a field experiment in which light conditions were manipulated for four months. Then, we linked our results to qualitative climate change scenarios for North-Patagonian forest predicting how future climate change will affect primary producers and periphyton stoichiometry in low-order streams through modifications in the structure of canopied zones. Finally, we found that biomass, photosynthetic parameters and the elemental content of periphyton exhibited a bell-shaped relationship with light availability which was, in turn, dependent on canopy cover. These trends are characterized by an increase from low light up to 250 μmol m^{-2} s^{-1} and a decline when light is over 750 μmol m^{-2} s^{-1}. Thus, intermediate light resulted in optimal conditions for primary producers' photosynthesis; however, these intermediate canopied zones are predicted to decrease in the future. Therefore, we predict changes in stream ecosystem stoichiometry due to variations in primary producers' photosynthesis, and, consequently, periphyton elemental composition as an outcome of forest structure modifications due to climate change.

Key words: canopy; primary producers; photosynthesis; periphyton; stoichiometry; Nothofagus; climate change.

Introduction

Riparian zones are major components of stream ecosystem function since they act as donors for organic matter processing (that is, the River Continuum Concept (Vannote and others 1980) and nutrient recycling [that is, the Nutrient Spiraling Concept (Webster and Patten 1979)]. The structure of the riparian canopy is dynamic, influencing the physical, chemical, and biological dimensions of

Received 2 November 2015; accepted 10 April 2016;
published online 2 June 2016
Electronic supplementary material: The online version of this article (doi:10.1007/s10021-016-9996-8) contains supplementary material, which is available to authorized users.
Author contribution Nicolás Martyniuk designed the study, performed research, analyzed data, and wrote the paper. Beatriz Modenutti designed the study, analyzed data, and wrote the paper. Esteban Balseiro designed the study, analyzed data, and wrote the paper.
*Corresponding author; e-mail: nmartyniuk@comahue-conicet.gob.ar

streams and mediating a number of terrestrial-aquatic linkages (Sweeney 1992). Forest–stream interactions can be better understood by analyzing these dynamics that control light availability in streams (Stovall and others 2009). The distribution of vertical foliage in riparian vegetation, its horizontal structure (e.g., its patchiness), and the species composition determines the light environment (Montgomery and Chazdon 2001). In addition, light regimes change when deciduous trees species in riparian zone gain leaves in the spring and lose leaves in autumn (Hill and Dimick 2002). Complex canopies often modify light availability by creating low-angle sun flecks that originate from spatially offset canopy gaps. Canopy cover can also vary over time in relation to forest development, the history of disturbances (e.g., fires and blowdown) (Gjerløv and Richardson 2010), and climate (O'Grady and others 2011; Williamson and others 2014).

In Earth's history, climate has played a major role in shaping the growth, composition, and genetic variation of vegetation across different landscapes (Williams and Dumroese 2013). Contemporary changes in our atmosphere have caused global mean temperature trends to increase at values previously experienced in geologic time (Marcott and others 2013); however, the velocity of change appears to be faster than that during similar periods (Williams and Dumroese 2013). Studies have indicated that forests of the world responded to regional climate variations by altering their range and density (Harsch and others 2009; Rehm and Feeley 2013). These shifts in vegetation composition and structure depend on seed dispersal (Rehm and Feeley 2013; Torres and others 2015), geographical barriers (Macias-Fauria and Johnson 2013), and climatic tolerance (Allen and others 2010). Susceptibility to climate change may result in the substitution of canopy species (Young and Leon 2007) and the extinction of particular tree species (Dirnböck and others 2011; Iglesias and others 2012). Therefore, canopy structure and dynamics are expected to be modified under climate change (O'Grady and others 2011; Svenning and Sandel 2013), and this will in turn influence stream periphyton.

Periphyton is defined as a matrix with a complex microorganisms community (algae, bacteria, fungi, protozoa, and small metazoan), organic and inorganic detritus that is attached to dead or living, organic or inorganic substrata (Wetzel 2001; Cross and others 2005). Autotrophs and microbial heterotrophs constitute the basal energy resources that support higher trophic levels in lotic food webs (Wetzel 2001). The carbon (C):nitrogen (N) and C:phosphorus (P) ratios of periphyton can vary considerably. These variations may be due to differences in the type of organic material with different elemental compositions (Frost and others 2002; Cross and others 2005; Frost and others 2005), variations in the composition of periphyton organisms (Frost and others 2005), or changes in the physiology of algae (Frost and others 2002, 2005; Hillebrand 2005). Studies in experimental streams revealed that light and phosphorus can have a positive effect on stream algae growth, depending on the irradiance level and the enrichment of nutrients (Hill and Fanta 2008; Hill and others 2009). The variation in light availability affects the photosynthetic process of aquatic primary producers. This modulates the carbon (C) fixation rate, which in turn affects the C:nutrient ratio (Sterner and others 1997). Under low-light conditions, primary producers increase their pigment content to maximize photosynthetic capacity and C fixation (Hill and others 2009). Under high light intensities and low levels of inorganic nutrients (primarily phosphorus and/or nitrogen), the biomass of primary producers disproportionately accumulates C relative to nutrients (Frost and others 2002; Sterner and Elser 2002). In addition, Xenopoulos and others (2002) reported that UVR also affects C:N and C:P of primary producers. Finally, if exposure to high-light conditions is prolonged in time C fixation is reduced due to photoinhibition (Takahashi and Murata 2008), consequently the C:nutrient ratio decreases due to a reduction in C fixation (Frost and others 2005; Martyniuk and others 2014).

Treelines are particularly sensitive to changes in temperature regimes (Harsch and others 2009) because the most pronounced changes in temperatures are expected at high altitudes and latitudes (Grigorév and others 2013). Changes in establishment, growth, and survival due to climate change have been described for treelines of different species in the Alps, Himalayas, and Rocky Mountains (Alaska) (Körner 2007; Randin and others, 2013). Thus, it can be predicted that treelines will move upwards (Harsch and others 2009; Donato 2013); however, regional changes in climate would determine the final treeline location (Macias-Fauria and Johnson 2013; Paulsen and Körner 2014). At a global scale, climate change will enhance open canopies with patches of closed forest (Svenning and Sandel 2013; Zhu and others 2014). Thus, the more sensitive ecosystems would be low-order streams located at the upper altitudinal limit of trees. In these ecosystems, substantial changes in

forest structure associated with downward and upward shifts in treelines are expected.

The North Patagonian Andes (at approximately 40°S) does not exceed 2500 m a.s.l.; treeline is located at approximately 1600 m a.s.l. (Villalba and others, 1997). The treeline near 40°S in Chile and Argentina is very dynamic and consists of the austral beech *Nothofagus pumilio* (Daniels and Veblen 2004). Previous studies have indicated that climate change will modify the treeline location because the establishment and growth of seedlings are highly dependent on rainfall seasonality (Magnin and others 2014; Álvarez and others 2015), summer temperature (Massaccesi and others 2007; Magnin and others 2014), and solar radiation (Martínez Pastur and others, 2011). Periods of drought/heat increase mortality, which will result in forest migration and/or retraction (Suarez and Kitzberger 2010). This forest dynamic will affect organic matter and nutrient input to North-Patagonian Andean streams (Díaz Villanueva and others 2016) that are characterized by very low nutrient concentrations (Pedrozo and others 1993; Modenutti and others 2010) and are free of anthropogenic pollution (Markert and others 1997). Here, we analyzed how *Nothofagus* forest structure will modify light availability and thus affect photosynthetic parameters and stoichiometry of periphyton of mountain streams. We carried out field sampling in streams with different canopies and conducted a field experiment in which light conditions were manipulated. We hypothesized that periphyton photosynthesis and stoichiometry in low-order streams will be affected by modifications in forest structure.

Methods

Study Streams

We sampled four mountain streams (Fresco, van Titter, Goye, and López) located at 41°S, 71°W in Nahuel Huapi National Park (Patagonia, Argentina) (Figure 1A). These streams receive water from precipitation and snow meltwater (total annual precipitation is 1500–2500 mm). The maxima discharges occur in May austral fall-winter (rain) and October spring (snowmelt); the lowest discharges occur in late summer (April). The substrate of all streams was dominated by boulders and cobbles. Headwaters are approximately located at 2000 m a.s.l. (Table 1). The low-order streams downhill are

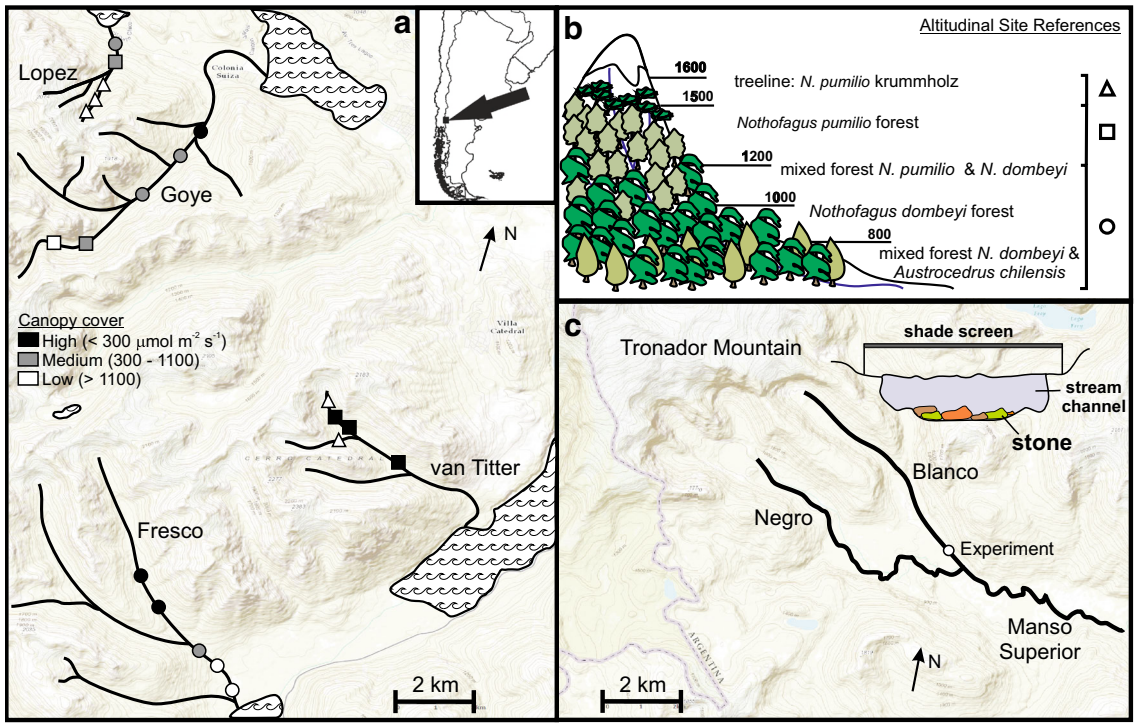

Figure 1. **A** Location of the four sampled streams and the positions of each sampled point. Note that every sampled point had a visual reference of canopy cover (light availability) and altitudinal composition of North Patagonian forest. **B** Scheme of altitudinal gradient of North Patagonian forest. **C** Location of experiment and its design.

Table 1. Physicochemical Parameters of van Titter, Fresco, Goye, and Lopez streams Measured on Five Sampling Points (±SD), and During Experiment on Blanco Stream

	Temperature (°C)	Turbidity (NTU)	TSS (mg l^{-1})	DOC (g l^{-1})	TDP (µg l^{-1})	TDN (µg l^{-1})	Conductivity (µS cm^{-1})	Dissolved Oxygen (mg l^{-1})	K_d (m^{-1})	HeadW (m)	Area (km^2)	MD (m)	FA (m)
van Titter	13.0 ± 2.1^{a}	0.6 ± 0.6^{b}	0.5 ± 0.1^{ns}	0.8 ± 0.4^{ns}	7.8 ± 1.0^{a}	122.6 ± 36.6^{a}	11.4 ± 1.9^{b}	11.1 ± 1.1^{ns}	0.7 ± 0.4	2100	14.6	978	3911
Goye	10.8 ± 0.6^{b}	0.4 ± 0.2^{b}	0.2 ± 0.1^{ns}	0.7 ± 0.1^{ns}	2.2 ± 0.9^{b}	84.1 ± 25.2^{a}	19.5 ± 7.0^{b}	9.8 ± 1.5^{ns}	0.3 ± 0.1	1945	32.2	1510	6038
Lopez	8.4 ± 0.9^{c}	0.7 ± 0.6^{b}	1.3 ± 1.4^{ns}	0.9 ± 0.5^{ns}	2.4 ± 0.7^{b}	55.6 ± 16.7^{b}	13.9 ± 9.5^{b}	9.7 ± 0.7^{ns}	0.2 ± 0.1	2027	4.34	643	2573
Fresco	9.0 ± 0.2^{c}	1.6 ± 0.2^{a}	0.5 ± 0.3^{ns}	0.7 ± 0.2^{ns}	3.3 ± 0.9^{b}	42.2 ± 12.7^{b}	42.9 ± 0.2^{a}	10.8 ± 3.3^{ns}	0.2 ± 0.2	1924	34.9	594	2377
ANOVA p value	$p = 0.004$	$p = 0.01$	$p = 0.11$	$p = 0.67$	$p < 0.001$	$p < 0.001$	$p < 0.001$	$p = 0.41$					
Blanco (experiment)	8.9 ± 1.8	4.1 ± 1.0	4.9 ± 2.3	0.4 ± 0.2	9.6 ± 4.8	51.3 ± 14.9	19.5 ± 1.8	9.7 ± 1.0	0.7 ± 0.3	1229	8.3		

We only show in the following table the results of comparisons between streams (a posteriori Tukey test); p values correspond to nested ANOVA
TSS total suspended solids, DOC dissolved organic carbon, TDN total dissolved nitrogen, TDP total dissolved phosphorus, K_d light extinction coefficient. The geographic parameters: HeadW headwater altitude, Area watershed area
Significant differences on Tukey test were under $p < 0.05$. Mean distance between sites (MD) and the distance between further afield sites (FA) were estimated among the same stream.

canopied by a stunted form (*krummholz*) of the deciduous austral beech *Nothofagus pumilio* (Villalba and others, 1997). Between elevations of 1200 and 1500 m, *N. pumilio* trees increase in importance and form dense and pure stands. At 1200–1000 m, the altitudinal belt vegetation changes to mixed stands with the evergreen species *Nothofagus dombeyi* (Veblen and others 1996). Bellow 1000 m, *N. dombeyi* dominates the temperate forest. At approximately 800 m, *N. dombeyi* is mixed with the Andean cedar *Austrocedrus chilensis*. The area is free of anthropogenic pollution and aerosol depositions (Markert and others 1997; Mladenov and others 2011).

During the summer (February–March 2014), we collected samples at 20 sampling sites (five at each stream, Figure 1). All streams were sampled within two weeks thus; we assumed a similar successional algal stage. These sites represented a wide range between open and closed riparian conditions along the studied streams (the stream widths were <10 m) (Table 1). Sampling stations that represent different types of riparian conditions were chosen based on aerial photographs (taken from Google Earth®) and preliminary visual observations. The dominant canopy species at these sites included the following three species: *N. pumilio*, *N. dombeyi*, and *A. chilensis* (Figure 1 B).

Sampling Procedures

At each sampling site, we measured turbidity (in nephelometric turbidity units; NTU) using a portable turbidity meter (Lutron TU-2016, Taipei, Taiwan). Temperature, conductivity, and dissolved oxygen were measured using an oxymeter-conductimeter (YSI 85, Ohio, USA). Each determination was carried out three times per site. We collected 1 l of stream water in acid-washed plastic containers, which were transported to the laboratory in thermally insulated containers for nutrient concentration measurements. In addition, four stones were randomly selected at each sampling site from a 6-m section of the main channel. On each stone surface, we determined the in situ periphytic photosynthetic parameters using a WATER-PAM (Heinz Walz GmbH, Effeltrich, Germany) equipped with a Water-EDF fiber optic unit. After being measured, each stone was individually stored in a plastic bag and immediately carried to the laboratory under dark conditions in thermally insulated containers. All the sampling stations at each stream were sampled on the same day.

Light Measurements

To measure the light environment over the canopied streams, we estimated the direct site factor (DSF) using digital hemispheric canopy photographs (Anderson 1964). The DSF is an approximation of the below-canopy light history at a specific site, which is associated with canopy openness (values range between 0-closed and 100-open). Hemispherical photographs were taken over the center of the stream channel using a CoolPix 995 digital camera (Nikon) equipped with a fisheye lens that provides a 180-degree view (FCE8, Nikon). The camera was mounted on a tripod set as low (<1 m) as possible over the surface of the water. The photographs taken during sampling were examined using WinSCANOPY™ software (Regent Instruments Inc., Canada) to calculate below-canopy light metrics. The light measurements were taken during the summer to reduce the effect of deciduous *N. pumilio* trees and different size leaves. Light measurements (five replicates) were taken within 2 h around noon.

Direct light (photosynthetic active radiation, PAR; that is, 400–700 nm) availability at the stream surface and at a depth of about 15 cm (stream bottom) was measured with an Armour SL-125 portable radiometer (Biospherical Instruments Inc., San Diego, CA, USA). The light attenuation coefficient (K_d) was calculated according to the following equation:

$$K_d = \frac{\ln(E_2/E_1)}{\Delta z}, \quad (1)$$

where E_2/E_1 is the ratio of irradiances at depth z_2 = 0.15 m to that at z_1 = 0; that is, the irradiance transmittance over depth interval $\Delta z = z_1 - z_2$. K_d was estimated from the direct light measurements (Table 1). Light measurements were expressed as available photosynthetic active radiation (PAR) at stream bottom in µmol photons m^{-2} s^{-1} (hereafter Underwater Light).

Photosynthetic Fluorescence Parameters

Photosynthetic parameters were measured in situ five times per stone at a saturating actinic light (SAL) measurement of 1004 µmol photons m^{-2} s^{-1} with a PAM-fluorometer. The fluorescence measurements started with F_0 (ground state, previous light conditions), which is the level of fluorescence of the antenna pigment (chlorophyll *a*) when all reactive centers of PSII are open. SAL was then applied, and the maximal fluorescence level was achieved (F_m). The steady-state value of fluorescence immediately prior to the flash is termed F_t. After a period of time, another SAL allowed for the estimate of the initial minimum fluorescence (F'_0) and maximal fluorescence (F'_m) (Maxwell and Johnson 2000).

All these fluorescence values were used to determine the following photosynthetic parameters (Mackey and others 2008; Rohácek and others 2008):

electron transport rate (ETR = µmol electrons m^{-2} s^{-1}),

photosynthesis efficiency $\left(Y = \frac{F'_m - F_t}{F'_m} = \frac{\Delta F}{F'_m}\right)$ of PSII (also known as PSII efficiency),

photochemical quenching $\left(qP = \frac{F'_m - F_t}{F'_m - F'_0}\right)$,

and non-photochemical quenching $\left(\text{NPQ} = \frac{F_m - F'_m}{F'_m}\right)$.

Increased light availability produces a reduction in the proportion of open reaction centers of PSII (qP). This change will be reflected in a decrease of the photosynthesis efficiency (*Y*) due to photoinhibition (light-induced damage on PSII), as well as a decrease in the electron transport rate (ETR) (Murata and others 2007). Therefore, the *Y*/qP ratio (that is the photosynthetic efficiency per open reactive center) will be low because there are great amounts of energy that will not be used by PSII. Contrariwise, the NPQ response is dependent on the light history of the organism (Müller and others 2001). NPQ is highly efficient in case of short-term light stress, but under prolonged high-light conditions is less relevant. Changes that occur in thylakoid membrane generate reactive oxygen species (ROS) that inhibit the repair of PSII by suppressing the synthesis of proteins (Murata and others 2007; Yamamoto and others 2014).

Laboratory Procedures

A 500 ml aliquot of stream water from each sampling site was filtered through ashed GF/F filters approximately 0.7 µm pore size. Total dissolved phosphorus (TDP), total dissolved nitrogen (TDN), and dissolved organic carbon (DOC) were determined for the filtered stream water. DOC and TDN were measured with a carbon–nitrogen analyzer (Shimadzu TOC-VCSH, with TN- M1, Kyoto, Japan). The samples used for TDP measurements were digested with potassium persulfate at 125°C at 1.5 atm for 1 h; the concentrations were analyzed using the ascorbate-reduced molybdenum method (Eaton and others 2005). The total suspended solids (TSS) were quantified by filtering 500 ml of stream water through pre-weighed GF/F filters, which were dried for at least 48 h at 60°C and then reweighed.

Periphyton was obtained by scraping the individual stones with a brush and rinsing them carefully with distilled water in the same day of sampling. The final volume obtained was adjusted to a constant volume (100 ml); the area (cm^2) scraped on the stone was estimated from the lengths of the three main axes (Graham and others 1987). This volume was designated for the estimation of chlorophyll *a* (Chl-*a*), C, and P concentrations based on one filter for each determination and analyzing in all cases the whole filter. To determine the Chl-*a* concentration, a 1-ml aliquot of the periphyton suspension was filtered through glass fiber filters (GF/F, Whatman™, Maidstone, UK). After the filtration step, Chl-*a* was extracted in hot ethanol (Nusch 1980) and measured with a 10-AU fluorometer (Turner Designs, Sunnyvale, CA, USA) previously calibrated against spectrophotometric measurements. Another 5 ml of the suspension was filtered through ashed GF/F filters, dried at 60°C for 48 h, and analyzed for particulate C using a Thermo Finnigan EA 1112 CN elemental analyzer (Thermo Scientific, Milano, Italy). The periphyton P concentration was determined by filtering another 5 ml of the suspension through acid-washed (10% HCl) and ashed GF/F filters, which were then dried at 60°C for 48 h. The filters were then combusted at 550°C for 1 h. The ashes were then placed in flasks, and the P concentrations were analyzed using the ascorbate-reduced molybdenum method (Eaton and others 2005). Periphyton Chl-*a*, C, and P concentrations were reported as mg m^{-2}. Each parameter was estimated using 4 replicates (4 stones per site).

Field Experiment

The field experiment was designed to measure periphyton responses to manipulated light conditions in a free canopy stream using a neutral shade screen. The experiment was located at Blanco stream (920 m.a.s.l., Figure 1C; Table 1) and conducted over 106 days during austral summer (December 2013–April 2014). The following two treatments were performed: full light (mean irradiance of 1729 µmol m^{-2} s^{-1}, up to 2414 µmol m^{-2} s^{-1} at noon during sunny days) and low light (neutral shade screen; mean irradiance of 335 µmol m^{-2} s^{-1}, up to 497 µmol m^{-2} s^{-1} at noon). The low-light treatment was achieved using a neutral screen that covered the entire width of the stream and 15 m in length. The screen was placed 15 cm above the stream surface and fixed with metal pegs 1 m away from the stream margin. This experiment was carried out during the period of low water flow (summer), and no hydrological changes (HOBO datalogger) were observed during the experiment. Daily light measurements were obtained from a meteorological station located 20 km from the experiment site and were corrected by periodically (every 2 weeks) direct measurement.

During the experiment, TDN, DOC, TSS, conductivity, turbidity, temperature, and dissolved oxygen were measured (Table 1). Stream temperatures and water levels were recorded using a data logger (U20 HOBO; Onset, Bourne, MA, U.S.A.). On five sampling occasions, we randomly selected four stones per treatment (full-light and low-light treatments). We estimated the in situ photosynthetic parameters (qP, Y, NPQ, Y/qP, and ETR) for each stone using a WATER-PAM equipped with a Water-EDF fiber optic unit. We collected each stone individually in a thermally insulated plastic container and immediately transported it to the laboratory under dark conditions. In the laboratory, substrata were scraped as previously described and the same parameters were then estimated.

Statistical Analysis

We compared the two methods of light measurement (that is, radiometer and hemispherical photography measurements) which were used to determine canopy openness and underwater (15 cm depth) light availability. We carried out two-way ANOVA to analyze the light availability among sites ($N = 5$) and streams ($N = 4$). A cluster analysis was used to group similar light conditions. Based on these results, we established three levels of canopy cover corresponding to light intensity. Each sampling point was classified using one of these levels. We then applied nested ANOVA and an a posteriori Tukey's test using R (Team 2015) to compare the limnological features (TSS, DOC, TDP, TDN, conductivity, turbidity, temperature, and dissolved oxygen) of the streams, with sampling points nested to streams. Each sampling point was a mean of four replicates (stones).

We generated Generalized Linear Mixed Models (GLMM) that assumed a normal error distribution with a log link function using R (Team 2015) to relate periphyton to the obtained variables: geographic course of the stream, altitude, turbidity, DOC, TDP, TDN, temperature, conductivity, dissolved oxygen, and radiance. We considered all the obtained variables and not highly correlated with each other (with Pearson's product-moment correlations among environmental variables <0.60). We considered all combinations of the seven predictors and the streams as a random factor with

four levels (to address the non-independence of data within each stream). We selected the model that best described primary producer biomass (Chl-*a* concentration) and applied Akaike's information criterion (AIC). For each model, we calculated the corrected AIC (AICc) value, which measures the model fit while correcting for small sample sizes. All the candidate models were ranked according to their AICc value, with the best model having the smallest AICc value. We then calculated ΔAICc, which is the difference between each model and the best-fit model within the model set. We used a set of the best supported models based on a model criterion of ΔAIC less than 2. After we determined the variable/s that were meaningful for the periphyton primary producers, we analyzed the relationship between the variable/s of the model with best AICc value and the response variables (that is, periphyton C, Chl-*a* concentration, periphyton C:P ratio, and photosynthetic parameters). We explored the relationships using Pearson's correlations; when significant relationships were found, we performed linear regressions and curve fitting. In all cases, normality and homoscedasticity were previously verified.

Results

Streams

The different sampling sites along the four sampled streams differed in canopy cover (DSF ranged from 10 to 98) and underwater light availability (57–2589 μmol m^{-2} s^{-1}, Figure 1). Light availability varied significantly among sites (two-way ANOVA, $F_{4,12} = 10.8$, $p < 0.001$). The cluster analyses (see Supplementary Material, S1) between stream sites revealed the following three groups according to underwater light conditions and canopy cover of sampling sites: low-light availability (from 0 to 300 μmol m^{-2} s^{-1}, high canopy), intermediate-light availability (from 300 to 1100 μmol m^{-2} s^{-1}), and high-light availability (from 1100 to 2600 μmol m^{-2} s^{-1}, low canopy). We compared direct measurements of underwater light (15 cm depth, log transformed) with measurements of below-canopy light (DSF) and found a significant correlation between both parameters (linear regression, $r^2 = 0.90$, $n = 20$, $F_{1,19} = 163.5$, $p < 0.001$). Therefore, the light availability represented different canopy covers. The understory light resulted from canopy cover as we did not find differences in light measurements between *N. pumilio* and *N. dombeyi* canopies. The total suspended solid (TSS) and dissolved organic carbon (DOC) concentrations were low (Table 1) and did not affect light availability.

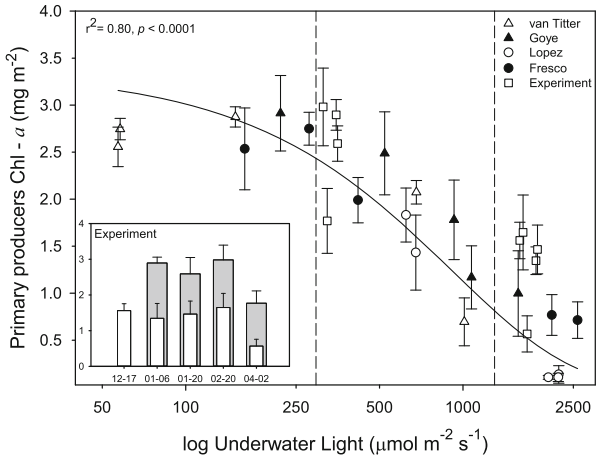

Figure 2. Relationship between periphyton Chl-*a* concentration and underwater light (15 cm depth). Data are given as the mean (four replicates -stones-) and standard error. *Nested graph* experimental results by sampled date (month-day): low-light (*gray*) and full-light (*white*) treatment. All treatment differences were significant at $p < 0.001$. *Vertical lines* show the 3 groups of light/-canopy.

Other limnological variables did not differ among sampling streams and sites. All streams exhibited low values of turbidity (0–1.82 NTU) and conductivity (11–42 μS cm^{-1}) (Table 1). However, the Fresco stream presented significantly higher tur-

Table 2. Best Approximating Models (ΔAIC < 2) for Predicting Periphyton Biomass (chlorophyll *a*) in Mountain Streams (van Titter, Fresco, Goye, and Lopez)

Model-variables	r^2	AIC_C	ΔAIC	w_i	*K*
Underwater light (UL)	0.62	38.130	0	0.383	1
UL + turbidity	0.65	39.134	1.004	0.141	3
UL + temperature + turbidity	0.71	39.918	1.788	0.092	3

Intercept and error terms were also included in all models
AIC Akaike's Information Criterion. k indicates the number of parameters. ΔAICc is the difference between the AICc value and the lowest AICc value. w_i is the relative likelihood that the model is the best approximating model.

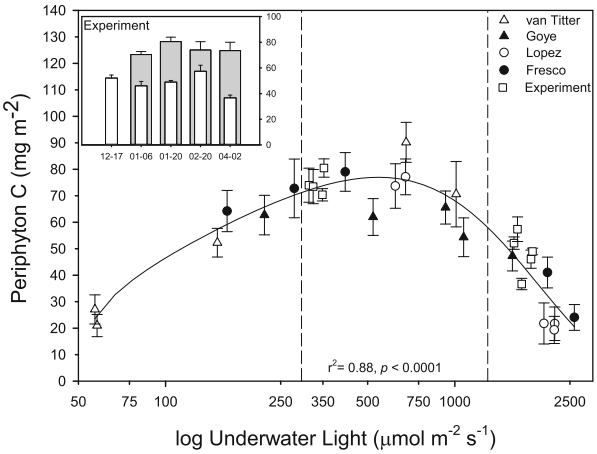

Figure 3. The relationship between periphyton C concentration and underwater light (15 cm depth) showed a bell-shaped curve. Data are given as the mean (four replicates -stones-) and standard error. *Nested graph* experimental results by sampled date (month-day): low-light (*gray*) and full-light (*white*) treatment. All treatment differences were significant at $p < 0.001$. *Vertical lines* show the 3 groups of light/canopy.

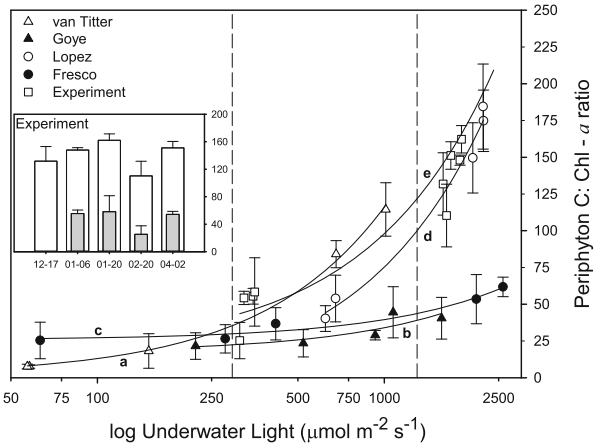

Figure 4. Relationship between periphyton C:Chl-*a* ratio and underwater light (15 cm depth). Linear regressions: ***a*** Lopez ($r^2 = 0.99$, $p = 0.0007$), ***b*** van Titter ($r^2 = 0.99$, $p < 0.0001$), ***c.*** Fresco ($r^2 = 0.96$, $p = 0.003$), ***d*** Goye ($r^2 = 0.72$, $p = 0.04$) and ***e.*** Experiment ($r^2 = 0.93$, $p < 0.0001$). Data are given as the mean (four replicates -stones-) and standard error. *Nested graph* experimental results by sampled date (month-day): low-light (*gray*) and full-light (*white*) treatment. All treatment differences were significant at $p < 0.001$. *Vertical lines* show the 3 groups of light/canopy.

bidity values (nested ANOVA, $F_{3,10} = 9.31$, $p = 0.003$; a posteriori Tukey's tests between all pairs were significant at $p < 0.05$) and conductivity values (nested ANOVA, $F_{3,10} = 53.6$, $p < 0.001$; a posteriori Tukey's tests between all pairs were

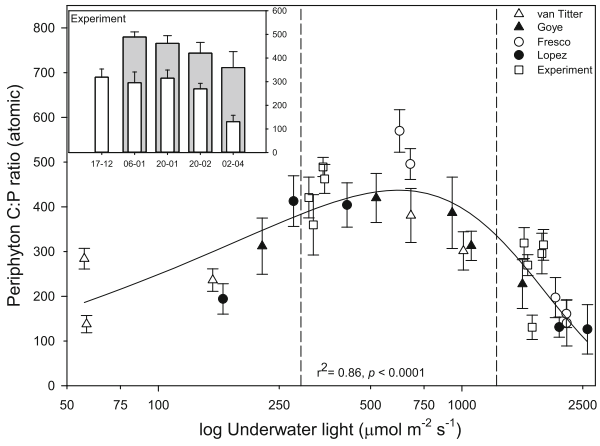

Figure 5. The relationship between periphyton C:P (atomic) and underwater light (15 cm depth) showed a bell-shaped curve. Data are given as the mean (four replicates -stones-) and standard error. *Nested graph* experimental results by sampled date (month-day): low-light (*gray*) and full-light (*white*) treatment. All treatment differences were significant at $p < 0.001$. *Vertical lines* show the 3 groups of light/canopy.

significant at $p < 0.001$). Canopy cover did not affect turbidity (nested ANOVA, $F_{2,10} = 2.8$, $p = 0.11$) nor conductivity ($F_{2,10} = 2.2$, $p = 0.16$). No differences in DOC values (Table 1) were observed among streams (nested ANOVA, $F_{3,10} = 0.4$, $p = 0.67$) or canopy levels (nested ANOVA, $F_{2,10} = 0.41$, $p = 0.73$). The concentrations of total dissolved phosphorus (TDP) were also low (<8 μg l^{-1}) in all streams (Table 1); the canopy cover did not affect P concentration (nested ANOVA, $F_{2,10} = 0.6$, $p = 0.55$). Total dissolved nitrogen (TDN) was high in van Titter and Goye (Table 1, nested ANOVA, $F_{3,10} = 30.3$, $p < 0.001$), but canopy cover did not affect TDN (nested ANOVA, $F_{2,10} = 0.7$, $p = 0.58$). The TDN:TDP ratio of streams ranges from 28 to 85. The water temperature was low, ranging between 8 and 13°C; there were significant differences in temperature among streams (nested ANOVA, $F_{3,10} = 8.5$, $p = 0.004$, Table 1).

Periphyton Biomass and Elemental Ratios

Periphyton Chl-*a* concentrations were higher (nested ANOVA, $F_{2,10} = 35.4$, $p < 0.001$) under low-light availability (high canopy cover, 2.9 mg Chl-*a* m^{-2}) than intermediate-light conditions (1.6 mg Chl-*a* m^{-2}), and sites with high-light availability (open canopy, 0.5 mg Chl-*a* m^{-2}). No differences were found among streams (nested ANOVA, $F_{3,10} = 1.13$, $p = 0.38$). To elucidate the main factors that control primary producer's bio-

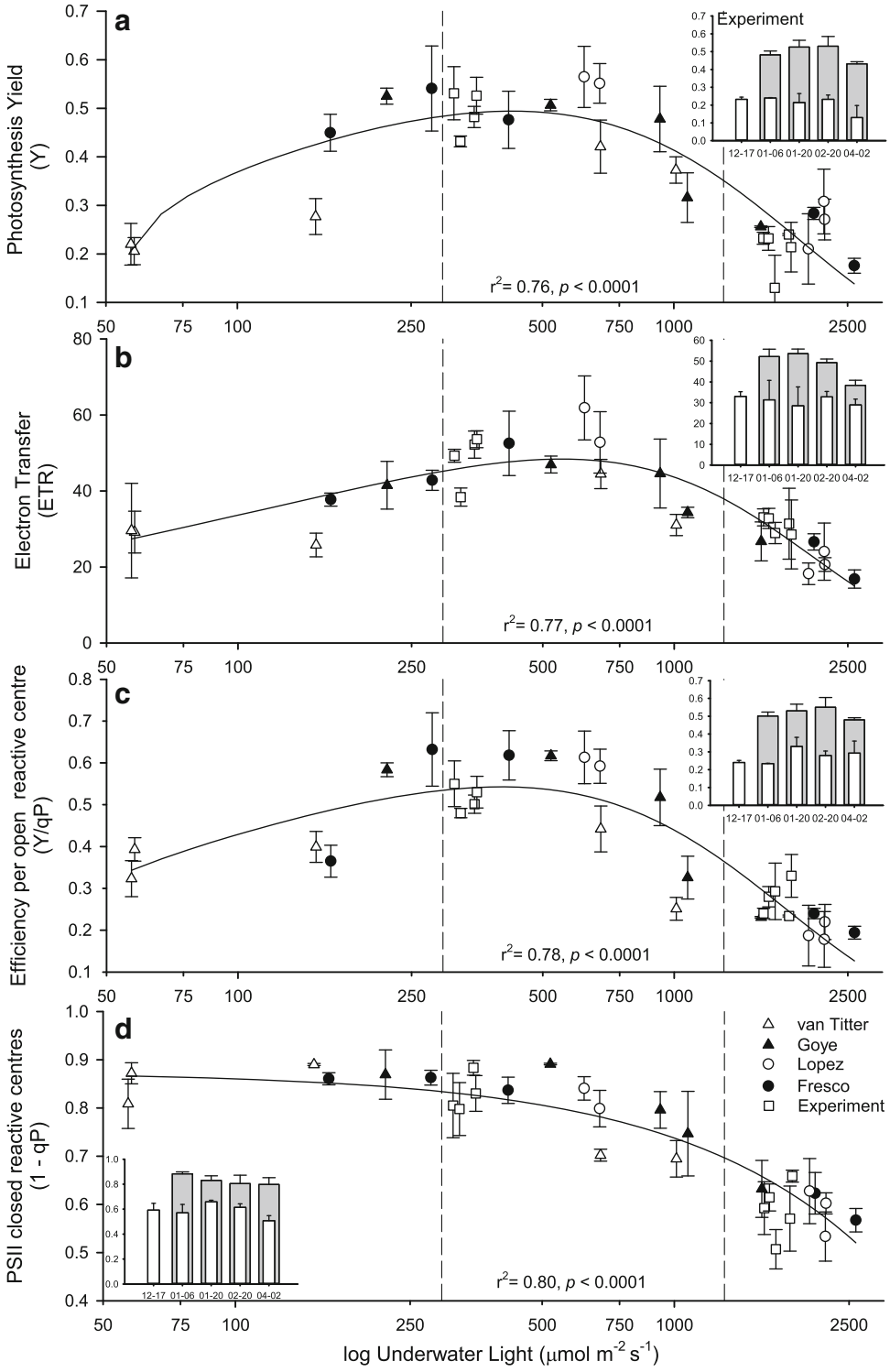

Figure 6. Responses of photosynthetic parameters to underwater light (15 cm depth). **A** Photosynthetic yield, **B** electron transfer (ETR), **C** photosynthetic efficiency per open reactive center (Y/qP), **D** PSII closed reactive centers (1-qP). Data are given as the mean (four replicates - stones-) and standard error. *Nested graph* experimental results by sampled date (month-day): low-light (*gray*) and full-light (*white*) treatment. All treatment differences were significant at $p < 0.05$. *Vertical lines* show the 3 groups of light/canopy.

mass (reflected in Chl-*a* values), we developed several environmental models. The models depicted in Table 2 were derived using a mixed model method, with streams included as a random variable. We obtained 127 environmental models. However, only 3 were supported by our data (ΔAIC < 2, Table 2) that explain the variations in Chl-*a* concentration. Among the different factors tested, light availability accounted for the higher likelihood model (Table 2) with an exponential decay curve fit ($r^2 = 0.80$, d.f. = 28, $p < 0.0001$) (Figure 2).

Only sites showed differences in periphyton C concentration (nested ANOVA, $F_{2,10} = 18.9$, $p = 0.0004$), due to differences in canopy cover and therefore in light availability. Sites under high- and low-light availability had periphyton C contents 1.4 and 2.5 times less, respectively, than that in sites with intermediate canopy cover (intermediate light availability). Thus, the periphyton C content in relation to light availability exhibited a bell-shaped curve (Figure 3) with maximum occurring between about 250 and 750 μmol m^{-2} s^{-1}. The relationship between periphyton C content and primary producers Chl-*a* (C: Chl-*a* ratio) showed that C:Chl-*a* ratio increased as canopy cover decreased (light availability increases). We found differences among sites (nested ANOVA, $F_{2,10} = 10.2$, $p = 0.004$), high-light availability had high C:Chl-*a* ratio than low- and intermediate-light availability (a posteriori Tukey's tests between all pairs were significant at $p < 0.01$). Intermediate- and low-light availability had no differences in C:Chl-*a* ratio (a posteriori Tukey, $p = 0.97$). Also each stream showed a particular relationship (nested ANOVA, $F_{3,10} = 4.4$, $p = 0.03$); this ratio differed among streams (e.g., the ratio ranged from 40 to 184.5 at Lopez and from 21.5 to 40.5 at Goye) (note different lines in Figure 4).

Due to differences in periphyton C contents and similarities in P contents (ANOVA, $F_{3,10} = 1.8$, $p = 0.21$), the periphyton C:P ratio exhibited a similar bell-shaped curve in relation to canopy cover (Figure 5). The maximum C:P ratio, which occurred 250 and 750 μmol m^{-2} s^{-1} and was consistent with that observed in the relationship between light and periphyton C (Figure 3).

Photosynthetic Parameters

We observed the highest photosynthesis yield (Y) under 250–750 μmol m^{-2} s^{-1} (Figure 6 A); the maximum electron transfer rate was also obtained under these conditions (Figure 6B). However, primary producers that were chronically exposed to high-light conditions (located under a low canopy with high-light conditions) showed low electron transfer rates. These decreases in electron transfer rates were also obtained under low-light conditions (high canopy cover).

Light quantity directly affects the photosynthetic mechanism. This was evident when we analyzed the photosynthetic efficiency per open reactive center of photosystem II (Y/qP, Figure 6C). The highest efficiencies were found in sites with light conditions between 250 and 750 μmol m^{-2} s^{-1}. The lowest efficiencies were observed in stream segments that were open or highly covered (high- and low-light availability). Primary producers under both light availability extremes exhibited similar responses (Figure 6). The photosynthetic machinery experiences these differences under high light as photosystem II is severely affected by chronic exposure to excessive light. During the PAM measurements, the actinic light pulse transiently closes all the reaction centers of PSII and provides a maximal fluorescence value in a light-adapted state (growth light). We found that the proportion of closed reactive centers (1-qP) increases when primary producers are adapted to low-light environments (Figure 6D). These organisms dissipate excess light as heat through NPQ (negative lineal regression between NPQ and light availability, slope = −0.09, $r^2 = 0.67$, $F_{1,28} = 54.2$, $p < 0.001$). This implies that excitation with excess light closes the reactive centers and dissipates heat. In contrast, autotrophs adapted to high-light conditions had low photosynthetic responses to the actinic pulse in all photosynthetic parameters (ETR, Y/qP, and 1-qP) (Figure 6).

Experimental Results

During the 106 days of the experiment, temperatures varied between 12.3 and 6.9°C, with an average temperature of 8.9 ± 1.8°C. Nutrient concentration remained almost invariable (Table 1).

Under low-light treatment, the light conditions were similar (mean = 335 μmol m^{-2} s^{-1}) to those found in the field at sites with intermediate light availability. In contrast, full-light treatment provided high-light (mean = 1729 μmol m^{-2} s^{-1}) across the experiment that was similar to streams with open canopies. Between low- and high-light treatments, significant differences in Chl-*a* concentrations (2.68 and 1.36 mg m^{-2}, respectively; two-way ANOVA, $F_{1,24} = 133.2$, $p < 0.001$, Figure 2), C contents (two-way ANOVA, $F_{1,24} = 31.5$, $p < 0.001$, Figure 3), and C:P ratios (two-way ANOVA, $F_{1,24} = 26.3$, $p < 0.001$, Figure 5) were observed. Under low-light treatment, a higher electron transfer rate was observed (two-way ANOVA, $F_{1,24} = 7.4$, $p = 0.012$, ETR = 48.38, Figure 6B). Accordingly, a higher photosynthetic rate was also observed under low-light treatment (two-way ANOVA, $F_{1,24} = 10.2$, $p = 0.004$, $Y = 0.5$, Figure 6A). The periphyton under the shaded treatment responded to SAL with a higher proportion of closed reactive centers (two-way ANOVA, $F_{1,24} = 6.8$, $p = 0.015$, 1-qP = 0.80, Figure 6D) and greater dissipation through heat (two-way ANOVA,

$F_{1,24}$ = 9.5, p = 0.005, NPQ = 0.26) than periphyton under high-light treatment (1-qP = 0.60, NPQ = 0.15). Furthermore, the obtained experimental data fit well with the field data. Therefore, these data were included in the figures relating light availability with periphyton parameters (see the empty squares in Figures 2, 3, 4, 5, 6 and the nested graphs with the differences between treatments during sampling dates).

Discussion

Here, we showed how *Nothofagus* riparian canopy affects the light environments of mountain streams in northern Patagonia. Changes in these environments affect primary producers biomass, photosynthetic parameters, and periphyton stoichiometry (C:P ratios). Our data suggest that the complexity of the forest structure directly affects periphyton stoichiometry. Light impacts photosynthesis, which in turn affects carbon fixation and elemental ratios. Light availability over streams was observed to be directly related to the vertical and horizontal complexity in forest structures (Stovall and others 2009). The spatial and temporal variations in irradiance occur when direct sun penetrates small openings in the canopy (sunflecks) (De Nicola and others 1992). When determining photosynthetic parameters with the PAM, the actinic pulse causes a change in light intensity that emulates a sunfleck penetrating through the canopy. We observed that periphyton communities growing under high-light conditions are light-stressed. Low photosynthetic responses were observed for all photosynthetic parameters (ETR, Y/qP, 1-qP) during the SAL pulse (Figure 6). Different studies have detected decreases in the response to spatial and temporal variations in irradiance in primary producers under light stress (Derks and others 2015) and a delay in the electron transport between PSII and PSI (Khatoon and others 2009). This process would interfere with the NPQ mechanism (Yamamoto and others 2014), increasing the susceptibility of the photosynthetic machinery to photodamage (Murata and others 2007). If this over-exposure is prolonged, the photochemistry of PSII will lose functionality and efficiency (Chan and others 2013) due to chronic photoinhibition (Derks and others 2015). However, periphyton exposed to low-light conditions also exhibited low photosynthetic parameters (Figure 6) during the SAL pulse. Because these periphytic autotrophs are growing under low-light conditions, they may have high susceptibility to sudden changes in irradiance (that is, sunflecks or SAL pulses). This extra energy cannot be used because the PSII reaction centers are closed to prevent photodamage, which increases heat dissipation. Previous studies have suggested that primary production increase monotonically with light availability with a plateau between 100 and 400 μmol m^{-2} s^{-1} (Hill and others 1995; Hill and Fanta 2008; Hill and others 2009). Hill and others (2009) employed a range of irradiances that are common in shaded streams, and found that the instantaneous irradiance that saturated growth was 100 μmol m^{-2} s^{-1}. Our results showed a bell-shaped trend with light-saturation point about 250 μmol m^{-2} s^{-1} and a decline point about 750 μmol m^{-2} s^{-1}. The difference in light saturation (100–400, 250–750 μmol m^{-2} s^{-1}) can be attributed to the light history of field primary producers that are exposed to variable and higher irradiances throughout the day than indoor experiments (Hill and Fanta 2008; Hill and others 2009) with controlled and constant light conditions. The change in the trend from an increase to a maximum to a bell-shaped response has important consequences when predicting the response of periphytic primary producers to changes in ambient light conditions.

The ratio of periphyton C to Chl-*a* may indicate the importance of primary producers relative to heterotrophic and detrital content (Geider 1987; Goedkoop and Johnson 1996). C:Chl-*a* ratios below 100 are values that indicate a high algal cellular content, whereas values up to 200 indicate a still significant contribution of algal cellular C to periphyton C (Geider 1987; Frost and others 2005). In our dataset, almost 69% of samples were under 100 and all samples (mean of 4 replicates) C:Chl-*a* ratios were below 200. Thus, our C:Chl-*a* measurements suggest that primary producers are functionally important in the periphyton matrix and our analysis of the photosynthetic parameters would reflect the dynamics of periphyton.

The observed changes in the photosynthetic parameters of primary producers have consequences in their elemental stoichiometry. Under low-light availability (high canopy cover) and because of light limitations, periphytic primary producers increase photon capture by maintaining a high proportion of open reactive centers (Figure 6D). Hill and Dimick (2002) studied the effect of seasonal changes in light availability on periphyton and found that light utilization efficiency was maximal under low-light conditions. This light limitation results in low C fixation, that affects the elemental composition of periphyton, resulting in a reduction in carbon content (low C:P and low C:Chl-*a* ratios) (Figure

s 3, 4, 5). In contrast under high-light conditions (low canopy cover) primary producers exhibited low Chl-*a* content (Figure 2) and high C:Chl-*a* ratio (Figure 3). These findings suggest that the size of the light-harvesting antennae was reduced (Croce and van Amerongen 2014) with a subsequent decrease in light-harvesting efficiency (Horton and others 2008). If this situation is prolonged, autotrophs can exude significant quantities of organic carbon (primarily as exopolymeric substances) (Rader and Belish 1997). A slow decomposition of this nutrient-poor organic matter would cause a reduction in the prevalence of algal cell (Frost and others 2002). Concurrently, heterotrophic bacteria and fungi associated with periphyton may become a significant carbon pool, decreasing the relative importance of algal biomass (Hillebrand and Kahlert, 2002). However, in our results most of the obtained C:Chl-*a* ratios were below 100 and all below 200 indicating a high importance of algal biomass in the periphyton matrix. Primary producers that remain under high-light–low-nutrient conditions have severely compromised their photosynthetic mechanism (low efficiency and low electron transport rate, Figure 6). Thus, a decrease in the C photosynthetic fixation results in a low C:P ratio (Figures 3, 5). In addition, the UVR component of sunlight also negatively affects the quantum yield and C fixation reducing the C:P ratio of periphyton (Xenopoulos and others 2002; Martyniuk and others 2014) and in experimental streams Frost and others (2007) found that UVB removal increased C:P ratio. In our study, canopy and the neutral screen of the field experiment decreased the solar spectra as a whole hence no differential absorption of different wavelengths can be assumed. Therefore, intermediate-light conditions of the whole solar radiation (PAR and UVR) resulted in optimal conditions for photosynthesis, as high ETR and high efficiency per open reactive center (Y/qP) were observed (Figure 6). These light conditions were achieved due to a combination of shade and sunflecks. Primary producers located under intermediate-light conditions benefitted from this fluctuating light.

Climate change predictions (Barros and others 2013; Magrin and others 2014) showed an increment in the probability of occurrence of extreme weather events (e.g., droughts and floods) that will modify scour, hydrology, and temperature regimes. Increases in air temperature will affect the quantity and timing of terrestrial detrital inputs relative to in situ aquatic production (Mulholland and others 2009). Also changes in scour and hydrology may increase runoff (Milly and others 2005) and this will produce modifications in allochthonous organic matter inputs (Kominoski and Rosemond 2012). Increased temperatures may promote microbial activity and nutrient sequestration (increasing detrital nutrient content) associated with organic matter and result in greater microbial than metazoan processing (Boyero and others 2011). Finally, reductions in the quantity and quality of terrestrial detritus and changes in autotrophs will alter production of microbial and metazoans in aquatic food webs (Kominoski and Rosemond 2012).

Forests also will respond to climate change by altering their range and density, resulting in shifts in vegetation structure (Suarez and Kitzberger 2010; Iglesias and others 2012). Based on the expected changes in precipitation and temperature in the North Patagonian wet forest (Barros and others 2013), we predict how these modifications may interact with periphyton parameters (Chl-*a*, periphyton C content, and photosynthetic parameters, Figure 6) considering that autotrophs are the main source of organic matter for periphyton. In the present situation, intermediate canopy cover allows for high Chl-*a* contents, high photosynthetic parameters, and high autochthonous C contents (through photosynthetic C fixation) across a wide sector (S2 A). However, in future scenarios (S2 B-C) of climate change derived from the IPCC and other studies climate change (Barros and others 2013) and of forest dynamics (Suarez and Kitzberger 2010; Iglesias and others 2012), the intermediate sector allowing for optimum conditions for periphyton development will be progressively reduced. In the near future (2015–2039), the light conditions for primary producers will change little; this is because the models predict small changes in forest structure at the treeline (Barros and others 2013). However, in the far future (2075–2099), the intermediate canopy cover is expected to retract (Daniels and Veblen 2004; Svenning and Sandel 2013; Zhu and others, 2014) because of an increase in extreme precipitation events and natural deforestation (Young and Leon 2007) reducing the optimum conditions for periphyton. These changes in forest structure may co-occur with other of the abovementioned hydrological and physical changes leading to complex and currently unexplored dynamics.

Alpine forest dynamics all around the world, including those in the Patagonian Andes, are expected to change due to climate conditions. Increased heat, floods, and drought will lead to a loss in forest cover (Palmer and others 2009; Williamson and others, 2014). However, in some pla-

ces, forests are shifting upwards (Donato 2013) and becoming more dense (Dial and others 2007). This would affect the development of optimum sectors for periphyton growth. Thus, it is important to consider that forests not only act as donors for stream ecosystems, as in the classic continuum stream models, but also modulate autochthonous carbon production through direct effects on light availability. Finally, it is necessary to develop climate change projections that consider the dynamics of riparian forest cover that will, in turn, affect stream ecosystem stoichiometry.

ACKNOWLEDGEMENTS

We thank to Paul Frost and one anonymous reviewer whose comments and suggestions greatly improved this manuscript. We thank the National Park Administration of Argentina for authorization to carry out this study. This work was supported by Fondo Nacional de Ciencia y Tecnica PICT 2012-1168 and PICT 2014-1002.

REFERENCES

Allen CD et al. 2010. A global overview of drought and heat-induced tree mortality reveals emerging climate change risks for forests. For Ecol Manag 259:660–84.

Álvarez C, Veblen TT, Christie DA, González-Reyes Á. 2015. Relationships between climate variability and radial growth of Nothofagus pumilio near altitudinal treeline in the Andes of northern Patagonia, Chile. For Ecol Manag 342:112–21.

Anderson M. 1964. Studies of the woodland light climate: I. The photographic computation of light conditions. J Ecol 52:27–41.

Barros VR, et al. 2013. Cambio climático en Argentina; tendencias y proyecciones. Barros VR, Vera C editors. Tercera Comunicacion de la República Argentina a la Convención Marco de las Naciones Unidas sobre Cambio Climático. Buenos Aires, Argentina: Centro de Investigaciones del Mar y la Atmósfera, Secretaria de Ambiente y Desarrollo Sustentable de la Nación, p 341.

Boyero L et al. 2011. A global experiment suggests climate warming will not accelerate litter decomposition in streams but might reduce carbon sequestration. Ecol Lett 14:289–94.

Chan T, et al. 2013. Quality control of photosystem II: lipid peroxidation accelerates photoinhibition under excessive illumination. PLoS One 7.

Croce R, van Amerongen H. 2014. Natural strategies for photosynthetic light harvesting. Nat Chem Biol 10:492–501.

Cross WF, Benstead JP, Frost PC, Thomas SA. 2005. Ecological stoichiometry in freshwater benthic systems: recent progress and perspectives. Freshw Biol 50:1895–912.

Daniels LD, Veblen T. 2004. Spatiotemporal influences of climate on altitudinal treeline in northern Patagonia. Ecology 85:1284–96.

De Nicola M, Hoagland KD, Roemer S. 1992. Influences of canopy cover on spectral irradiance and periphyton assemblages in a Prairie stream. J N Am Benthol Soc 114:391–404.

Derks A, Schaven K, Bruce D. 2015. Diverse mechanisms for photoprotection in photosynthesis. Dynamic regulation of photosystem II excitation in response to rapid environmental change. Biochim Biophys Acta 1847:468–85.

Dial RJ, et al. 2007. Changes in the alpine forest-tundra ecotone commensurate with recent warming in southcentral Alaska: evidence from orthophotos and field plots. J Geophys Res 112.

Díaz Villanueva V, Bastidas Navarro M, Albariño R. 2016. Seasonal patterns of organic matter stoichiometry along a mountain catchment. Hydrobiologia.

Dirnböck T, Essl F, Rabitsch W. 2011. Disproportional risk for habitat loss of high-altitude endemic species under climate change. Glob Change Biol 17:990–6.

Donato DC. 2013. Limits to upward movement of subalpine forests in a warming climate. Proc Natl Acad Sci USA 110:7971–2.

Eaton AD, et al. 2005. Standard methods for the examination of water and wastewater. Washington: American Public Health Association, American Water Works Association.

Frost P, Stelzer RS, Lamberti GA, Elser JJ. 2002. Ecological stoichiometry of trophic interactions in the benthos: understanding the role of C:N: P ratios in lentic and lotic habitats. J N Am Benthol Soc 21:515–28.

Frost PC et al. 2007. Effects of dissolved organic matter and ultraviolet radiation on the accrual, stoichiometry and algal taxonomy of stream periphyton. Freshw Biol 52:319–30.

Frost PC, Hillebrand H, Kahlert M. 2005. Low algal carbon content and its effect on the C:P stoichiometry of periphyton. Freshw Biol 50:1800–7.

Geider RJ. 1987. Light and temperature dependence of the carbon to chlorophyll a ratio in microalgae and cyanobacteria: implications for physiology and growth of phytoplankton. New Phytol 106:1–34.

Gjerløv C, Richardson JS. 2010. Experimental increases and reductions of light to streams: effects on periphyton and macroinvertebrate assemblages in a coniferous forest landscape. Hydrobiologia 652:195–206.

Goedkoop W, Johnson RK. 1996. Pelagic-benthic coupling: Profundal benthic community response to spring diatom deposition in mesotrophic Lake Erken. Limnol Oceanogr 41:636–47.

Graham AA, McCaughan DJ, McKee FS. 1987. Measurement of surface area of stones. Hydrobiologia 157:85–7.

Grigorév AA, Moiseev PA, Nagimov ZY. 2013. Dynamics of the timberline in high mountain areas of the nether-polar Urals under the influence of current climate change. Russ J Ecol 44:312–23.

Harsch MA, Hulme PE, McGlone MS, Duncan RP. 2009. Are treelines advancing? A global meta-analysis of treeline response to climate warming. Ecol Lett 12:1040–9.

Hill WR, Dimick SM. 2002. Effects of riparian leaf dynamics on periphyton photosynthesis and light utilisation efficienc. Freshw Biol 47:1245–56.

Hill WR, Fanta SE. 2008. Phosphorus and light colimit periphyton growth at subsaturating irradiances. Freshw Biol 23:215–25.

Hill WR, Fanta SE, Roberts BJ. 2009. Quantifying phosphorus and light effects in stream algae. Limnol Oceanogr 54:368–80.

Hill WR, Ryon MG, Schilling EM. 1995. Light limitation in a stream ecosystem: responses by primary producers and consumers. Ecology 76:1297–309.

Hillebrand H. 2005. Light regime and consumer control of autotrophic biomass. J Ecol 93:758–69.

Hillebrand H, Kahlert M. 2002. Effect of grazing and water column nutrient supply on biomass and nutrient content of sediment microalgae. Aquat Bot 72:143–59.

Horton P et al. 2008. Photosynthetic acclimation: does the dynamic structure and macro-organisation of photosystem II in higher plant grana membranes regulate light harvesting states? FEBS J 275:1069–79.

Iglesias V et al. 2012. Climate and local controls of long-term vegetation dynamics in northern Patagonia (Lat 41°S). Quat Res 78:502–12.

Khatoon M et al. 2009. Quality control of photosystem II: thylakoid unstacking is necessary to avoid further damage to the D1 protein and to facilitate D1 degradation under light stress in spinach thylakoids. J Biol Chem 284:25343–52.

Kominoski JS, Rosemond AD. 2012. Conservation from the bottom up: forecasting effects of global change on dynamics of organic matter and management needs for river networks. Freshw Sci 31:51–68.

Körner C. 2007. Climatic treelines: conventions, global patterns, causes. Erdkunde 61:316–24.

Macias-Fauria M, Johnson EA. 2013. Warming-induced upslope advance of subalpine forest is severely limited by geomorphic processes. Proc Natl Acad Sci USA 110:8117–22.

Mackey KRM, Paytan A, Grossman AR, Bailey S. 2008. A photosynthetic strategy for coping in a high-light, low-nutrient environment. Limnol Oceanogr 53:900–13.

Magnin A, Puntieri J, Villalba R. 2014. Interannual variations in primary and secondary growth of *Nothofagus pumilio* and their relationships with climate. Trees 28:1463–71.

Magrin GO, et al. 2014. Central and South America. In: Barros VR, Field CB, Dokken DJ, Mastrandrea MD, Mach KJ, Bilir TE, Chatterjee M, Ebi KL, Estrada YO, Genova RC, Girma B, Kissel ES, Levy AN, MacCracken S, Mastrandrea PR, White LL, Eds. Climate Change 2014: Impacts, adaptation, and vulnerability. Part B: regional aspects. Contribution of Working Group II to the Fifth Assessment Report of the Intergovernmental Panel on Climate Change. Cambridge, United Kingdom and New York, NY, USA: Cambridge University Press, pp 1499–566.

Marcott SA, Shakun JD, Clark PU, Mix AC. 2013. A reconstruction of regional and global temperature for the past 11,300 years. Science 339:1198–201.

Markert B et al. 1997. A contribution to the study of the heavy-metal and nutritional element status of some lakes in the southern Andes of Patagonia (Argentina). Sci Total Environ 206:1–15.

Martínez Pastur GJ et al. 2011. Canopy structure analysis for estimating forest regeneration dynamics and growth in *Nothofagus pumilio* forests. Ann Forest Sci 68:587–94.

Martyniuk N, Modenutti B, Balseiro E. 2014. Can increased glacial melting resulting from global change provide attached algae with transient protection against high irradiance? Freshw Biol 59:2290–302.

Massaccesi G, Roig FA, Martínez Pastur GJ, Barrera MD. 2007. Growth patterns of *Nothofagus pumilio* trees along altitudinal gradients in Tierra del Fuego, Argentina. Trees 22:245–55.

Maxwell K, Johnson GN. 2000. Chlorophyll fluorescence—a practical guide. J Exp Bot 51(345):659–68.

Milly PCD, Dunne KA, Vecchia AV. 2005. Global pattern of trends in streamflow and water availability in a changing climate. Nature 438:347–50.

Mladenov N et al. 2011. Dust inputs and bacteria influence dissolved organic matter in clear alpine lakes. Nat Commun 2:405.

Modenutti B et al. 2010. Structure and dynamic of food webs in Andean North Patagonian freshwater systems: organic matter, light and nutrient relationships. Ecol Aust 20:95–114.

Montgomery RA, Chazdon RL. 2001. Forest structure, canopy architecture and light transmittance in tropical wet forests. Ecol Eng 82:2707–18.

Mulholland PJ, Roberts BJ, Hill WR, Smith JG. 2009. Stream ecosystem responses to the 2007 spring freeze in the southeastern United States: unexpected effects of climate change. Glob Change Biol 15:1767–76.

Müller P, Li XP, Niyogi KK. 2001. Non-photochemical quenching. A response to excess light energy. Plant Physiol 125:1558–66.

Murata N, Takahashi S, Nishiyama Y, Allakhverdiev SI. 2007. Photoinhibition of photosystem II under environmental stress. Biochim Biophys Acta 1767:414–21.

Nusch EA. 1980. Comparison of different methods for chlorophyll and phaeopigment determination. Archiv für Hydrobiologie-Beiheft Ergebnisse der Limnologie 14:14–36.

O'Grady AP, Tissue DT, Beadle CL. 2011. Canopy processes in a changing climate. Tree Physiol 31:887–92.

Palmer MA et al. 2009. Climate change and river ecosystems: protection and adaptation options. Environ Manag 44:1053–68.

Paulsen J, Körner C. 2014. A climate-based model to predict potential treeline position around the globe. Alpine Botany.

Pedrozo F, Chillrud S, Temporetti P, Diaz M. 1993. Chemical composition and nutrient limitation in rivers and lakes of northern Patagonian Andes (39.5° -42°S; 71°W) (Rep. Argentina). Verh Int Verein Limnol 25:207–14.

Rader R, Belish T. 1997. Effects of ambient and enhanced UV-B radiation on periphyton in a mountain stream. J Freshw Ecol 12:615–28.

Randin CF et al. 2013. Do the elevational limits of deciduous tree species match their thermal latitudinal limits? Glob Ecol Biogeogr 22:913–23.

Rehm EM, Feeley KJ. 2013. Forest patches and the upward migration of timberline in the southern Peruvian Andes. For Ecol Manag 305:204–11.

Rohácek K, Soukupová J, Bartak M. 2008. Chlorophyll fluorescence: a wonderful tool to study plant physiology and plant stress. Plant Cell Compartments—Selected Topics 41–104.

Sterner RW, Elser JJ. 2002. Ecological stoichiometry: the biology of elements from molecules to the biosphere. Princeton: Princeton University Press, xxi

Sterner RW et al. 1997. The light: nutrient ration in lakes: the balance of energy and materials affects ecosystem structure and process. Am Nat 150:663–84.

Stovall JP, Keeton WS, Kraft CE. 2009. Late-successional riparian forest structure results in heterogeneous periphyton distributions in low-order streams. Can J For Res 39:2343–54.

Suarez ML, Kitzberger T. 2010. Differential effects of climate variability on forest dynamics along a precipitation gradient in northern Patagonia. J Ecol 98:1023–34.

Svenning JC, Sandel B. 2013. Disequilibrium vegetation dynamics under future climate change. Am J Bot 100:1266–86.

Sweeney BW. 1992. Streamside forests and the physical, chemical, and trophic characteristics of Piedmont streams in Eastern North America. Water Sci Technol 26:2653–73.

Takahashi S, Murata N. 2008. How do environmental stresses accelerate photoinhibition? Trends Plant Sci 13:178–82.

Team RDC. 2015. A language and environment for statistical computing. Vienna, Austria: R Foundation for Statistical Computing.

Torres AD et al. 2015. Seed production and recruitment in primary and harvested Nothofagus pumilio forests: influence of regional climate and years after cuttings. For Syst 24:016.

Vannote RL et al. 1980. The river continuum concept. Can J Fish Aquat Sci 37:130–7.

Veblen TT, Hill RS, Read J. 1996. The ecology and biogeography of Nothofagus forests. New Haven: Yale University Press.

Villalba R et al. 1997. Recent trends in tree-ring records from high elevation sites in the Andes of northern Patagonia. Clim Change 36:425–54.

Webster JR, Patten BC. 1979. Effects of watershed perturbation on stream potassium and calcium dynamics. Ecol Monogr 49:51–72.

Wetzel RG. 2001. Limnology : lake and river ecosystems. San Diego: Academic Press.

Williams MI, Dumroese RK. 2013. Preparing for climate change: forestry and assisted migration. J For 111:287–97.

Williamson GJ et al. 2014. Projecting canopy cover change in Tasmanian eucalypt forests using dynamically downscaled regional climate models. Reg Environ Change 14:1373–86.

Xenopoulos MA, Frost PC, Elser JJ. 2002. Joint effects of UV radiation and phosphorus supply on algal growth rate and elemental composition. Ecology 83:423–35.

Yamamoto Y et al. 2014. Quality control of PSII: behavior of PSII in the highly crowded grana thylakoids under excessive light. Plant Cell Physiol 55:1206–15.

Young KR, Leon B. 2007. Tree-line changes along the Andes: implications of spatial patterns and dynamics. Philos Trans R Soc Lond B Biol Sci 362:263–72.

Zhu K et al. 2014. Dual impacts of climate change: forest migration and turnover through life history. Glob Chang Biol 20:251–64.